WEP Warwick Evans Publishing

International Journal of Natural Resources and Environmental Studies

ISSN: 3006-2012 (Print), ISSN: 3006-0834 (Online) | Volume 8, Number 3, Year 2026
DOI: https://doi.org/10.62051/ijnres.v8n3.13
Journal homepage: https://wepub.org/index.php/IJNRES/index

Geochemical Characteristics and Geological Significance of Shale in Wufeng-Longmaxi Formations of Hefeng In Western Hunan-Hubei Underwater Uplift

Qiang Zhu*

The second Prospecting Team of Anhui Provincial Bureau of Coal Geology Wuhu, 241000, China
*Corresponding Author: Qiang Zhu (zhuqiang@home.hpu.edu.cn)

ABSTRACT

To elucidate the sedimentary environment and provenance background of the Wufeng–Longmaxi Formation in the Shuiquan area of Hefeng, Hubei Province, geochemical analyses were conducted on samples collected from an observed profile. The results indicate that the sedimentation of the Wufeng Formation occurred under predominantly cold and dry climatic conditions, whereas the Longmaxi Formation was characterized by a warm and humid climate. The ratios of Ba/Al and Ba(bio) suggest that the ancient productivity at the base of the Longmaxi Formation was relatively high. During its deposition, the Wufeng Formation experienced an oxidizing to sub-oxic environment, while the Longmaxi Formation exhibited an overall sub-oxic environment. Variations in rare earth elements indicate that the sedimentation rate of the Wufeng Formation was higher than that of the Longmaxi Formation; however, a layer with a significantly slow sedimentation rate is present at the base of the Longmaxi Formation; According to the U/Mo covariance model, the sedimentary environment of the Longmaxi Formation is characterized by a strong retention of water bodies. The characteristics of trace elements and rare earth element compositions and their ratios indicate that the material sources primarily originate from the upper crust, exhibiting a relatively homogeneous source with the main parent rock being felsic granite. The tectonic background of the source area is predominantly characterized by an active continental margin, while also displaying some features typical of continental island arcs.

KEYWORDS

Wufeng-Longmaxi Formation; Geochemical characteristics; Depositional environment; Ancient productivity.

1. INTRODUCTION

The Ordovician-Silurian transition is an eventful period in geological history. Many geological events have occurred, including volcanic events, glacial events, extinction of biological clusters and recovery events. At this stage, global shale is widely developed[1, 2].

Due to the continuous large-scale exploitation of conventional oil and gas, its resources are gradually difficult to support huge resource consumption[3]. Therefore, countries around the world have gradually turned their attention to unconventional oil and gas of shale gas. According to relevant research, it is shown that the organic-rich black shale of the Ordovician Wufeng Formation-Silurian Longmaxi Formation is widely developed in the Upper Yangtze region. It has the characteristics of favorable sedimentary facies, large thickness[4], high organic carbon content[5, 6], high maturity[7], pore micro-fracture development[8, 9], high brittle mineral content and high gas content[10-12]. It is

an important favorable exploration layer for shale gas. This discovery has prompted people to carry out a series of studies on the Wufeng-Longmaxi shale.

The sedimentary environment of Ordovician Wufeng Formation-Silurian Longmaxi Formation in the Middle-Upper Yangtze area varies greatly[13-15]. The analysis and judgment of its sedimentary characteristics and environment are the basis and important content of shale gas exploration and evaluation. The development control factors of organic-rich black shale, such as marine paleoproductivity, paleoclimate, redox environment of seawater, water retention and deposition rate, are reflected by elemental geochemical methods, and the sedimentary environment is inverted in order to provide more accurate basic data of organic-rich shale for shale gas exploration in Wufeng Formation-Longmaxi Formation.

2. GEOLOGICAL SETTING

The study area is located in the middle and upper Yangtze region from the Wufeng period of the late Ordovician to the Longmaxi period of the early and middle Silurian. It is surrounded by the Kangdian ancient land, the central Guizhou ancient uplift, the central Sichuan ancient uplift and the Xuefeng ancient uplift, forming a paleogeographic pattern of shallow sea deposits opening to the northeast[16-18]. The study area is located in the underwater highland uplift of western Hunan and Hubei on the northwest side of Jiangnan Xuefeng paleo-uplift.

During the sedimentary period of the Late Ordovician Wufeng Formation-Early Silurian Longmaxi Formation, the study area was in a shallow shelf sedimentary environment[15, 19]. Influenced by the Guangxi movement in Guangxi, the Cathaysia ancient land advanced to the northwest in stages, and the upper Yangtze platform was uplifted as a whole[20]. The emergence of paleo-uplifts in western Hubei may be related to the plate bending caused by the load of the Cathaysian plate on the Yangtze plate[21]. By the end of the Caledonian, the effect of the Guangxi movement on the middle Yangtze was weakened, resulting in the development of differential uplift in the study area, forming the paleo-underwater uplift in western Hunan and Hubei where the study area is located[22].

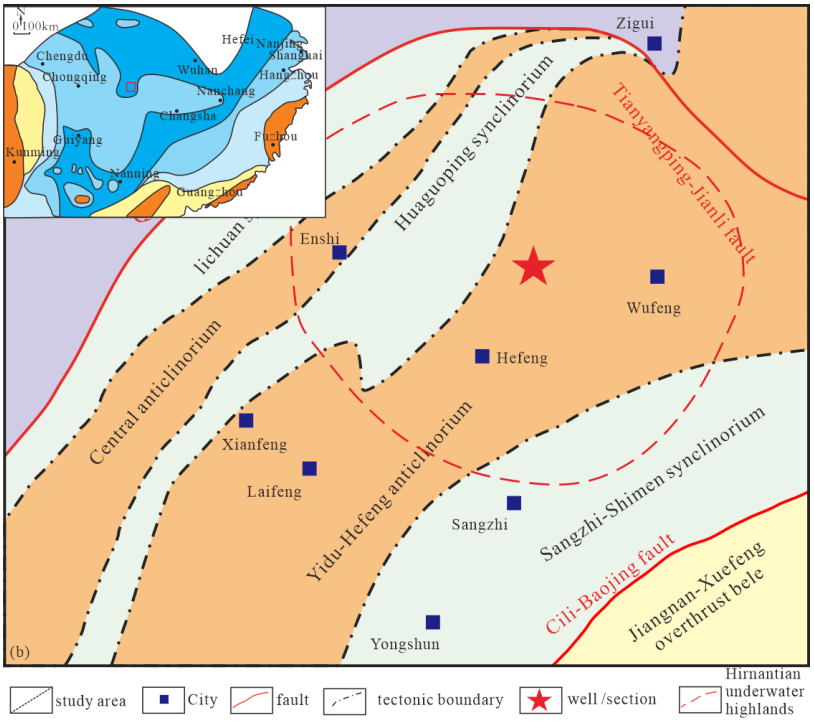

Figure 1 Regional structure and geographical location of the study area

After several stages of tectonic evolution in the study area, according to the regional tectonic characteristics, current tectonic features and previous research results, the western Hunan and Hubei

regions are further divided into Lichuan synclinorium, central synclinorium, Yidu-Hefeng anticlinorium and Sangzhi-Shimen synclinorium from northwest to southeast. The study area is mainly located in Yidu-Hefeng anticlinorium belt[23].

3. SAMPLES AND METHODS

The geochemical analysis of the sample was completed in the Australasia (Guangzhou) Mineral Laboratory. Before the test, the sample was ground to 200 mesh (0.074mm) in the agate ball mill. The main element test uses the Dutch PANalyticalPW2424 X-ray fluorescence spectrometer. The instrument X-ray tube operating voltage is 40 kV and the operating current is 70 mA. Trace elements and rare earth elements were tested and analyzed by POEMSIII plasma mass spectrometer, and the test accuracy was better than 5 %.

3.1. Chemical composition analysis

The element analysis table (Table 1) shows that the chemical composition of the Wufeng Formation-Longmaxi Formation in the study area is mainly SiO2, the content is between 60.93 % and 76.17 %, with an average of 67.46 %; followed by Al2O3 and TFe2O3, the average contents were 15.36 % and 4.18 %, respectively. The total content of these three main components ranged from 84.68 % to 89.93 %, with an average of 86.99 %. Compared with Na2O, K2O is more enriched, and its content is between 1.81 % and 5.42 %, with an average of 3.87 %. The chemical components of Wufeng group are mainly SiO2, CaO and Al2O3, and the average contents are 31.62 %, 27.27 % and 7.93 %, respectively. The total contents of these three components are between 63.19 % and 73.45 %. It shows that the rock composition of Wufeng Formation is mainly composed of quartz carbonate rock and a small amount of clay minerals, while the rock minerals of Wufeng Formation-Longmaxi Formation are mainly quartz and clay minerals, and clay minerals contain higher illite and chlorite minerals.

Table 1 Composition characteristics of major elements (μg/g) in rock samples of Wufeng Formation-Longmaxi Formation

Sample	Formation	Al_2O_3	BaO	CaO	Cr_2O_3	TFe_2O_3	K_2O	MgO	MnO	Na_2O	P_2O_5	SiO_2	SO_3	SrO	TiO_2	LOI
HSP-B1	Wufeng Formation	5.81	0.07	35.7	0.01	2.46	1.38	1.70	0.14	0.36	0.02	21.68	0.01	0.04	0.28	30.17
HSP-B2		12.72	0.16	15.30	0.01	4.13	3.42	2.01	0.05	0.50	0.04	45.43	0.09	0.02	0.60	14.91
HSP-B3		5.26	0.07	30.8	0.01	3.68	1.14	2.82	0.19	0.32	0.05	27.76	0.68	0.04	0.27	27.19
Mean Value		7.93	0.10	27.27	0.01	3.42	1.98	2.18	0.13	0.39	0.04	31.62	0.26	0.03	0.38	24.09
Minimum Value		5.26	0.07	15.30	0.01	2.46	1.14	1.70	0.05	0.32	0.02	21.68	0.01	0.02	0.27	14.91
Maximum Value		12.72	0.16	35.70	0.01	4.13	3.42	2.82	0.19	0.50	0.05	45.43	0.68	0.04	0.60	30.17
HSP-B4	Longmaxi Formation	19.68	0.27	0.12	0.01	3.36	5.42	1.86	0.02	0.67	0.05	63.06	1.70	0.01	0.90	4.66
HSP-B5		17.30	0.24	0.07	0.02	4.00	4.38	2.09	0.01	0.59	0.07	65.44	0.14	0.01	0.83	5.11
HSP-B6		17.46	0.31	0.14	0.02	3.45	4.48	1.72	0.01	0.63	0.08	66.12	0.10	0.01	0.86	5.08
HSP-B7		16.00	0.20	0.34	0.02	3.23	4.45	1.99	0.01	0.70	0.09	65.56	0.04	0.01	0.85	6.66
HSP-B8		14.80	0.19	0.25	0.02	3.48	4.05	1.90	0.01	0.56	0.13	66.40	0.05	0.01	0.85	6.87
HSP-B9		10.10	0.14	0.10	0.01	2.44	2.67	1.36	0.01	0.42	0.11	76.17	0.05	<0.01	0.54	5.20
HSP-B10		12.02	0.20	0.06	0.02	2.61	3.17	1.52	0.01	0.39	0.05	74.31	0.03	0.01	0.59	5.32
HSP-B11		11.14	0.18	0.07	0.02	1.95	2.85	1.26	0.01	0.78	0.12	75.03	0.06	<0.01	0.62	6.05
HSP-B12		17.94	0.17	0.09	0.02	5.19	4.31	2.29	0.04	0.92	0.08	63.33	1.85	0.01	0.68	5.05
HSP-B13		18.69	0.18	0.13	0.02	6.66	4.43	2.34	0.04	0.83	0.11	61.23	0.01	0.01	0.73	4.89
HSP-B14		18.81	0.16	0.14	0.02	6.07	4.46	2.23	0.03	0.84	0.10	60.93	0.01	<0.01	0.73	4.83
HSP-B15		10.34	0.11	0.09	0.01	7.70	1.81	1.38	0.05	1.47	0.13	71.89	5.94	0.01	0.49	3.78
Mean Value		15.36	0.20	0.13	0.02	4.18	3.87	1.83	0.02	0.73	0.09	67.46	0.83	0.01	0.72	5.29
Minimum Value		10.10	0.11	0.06	0.01	1.95	1.81	1.26	0.01	0.39	0.05	60.93	0.01	0.01	0.49	3.78
Maximum Value		19.68	0.31	0.34	0.02	7.70	5.42	2.34	0.05	1.47	0.13	76.17	5.94	0.01	0.90	6.87

3.2. Trace element characteristics

According to the results of trace element analysis in the study area (Table 2), compared with the abundance of trace elements in the upper crust[24], Ni, Mo, Ba and U elements in the Longmaxi Formation are moderately enriched, and the concentration coefficients are 2.0,2.4,2.6 and 2.1, respectively. Sc, V, Cr, Zn, Th and Zr elements are weakly enriched. The enrichment coefficients were 1.5,1.7,1.9,1.3,1.9 and 1.1, respectively. However, Co and Sr are strongly depleted, and the concentration coefficients are 0.4 and 0.1.

From the vertical variation diagram of trace element ratio (Fig.2), there are abnormal high values at the bottom of Longmaxi Formation. V/V+Ni and Ni/Co in the early trace element ratio index show a significant positive correlation, and V/Cr shows a significant negative correlation. The δU value is higher in the entire Longmaxi Formation than in the Wufeng Formation, and the change is gentle in the Longmaxi Formation.

Table 2 Composition characteristics of trace elements (μg/g) in rock samples of Wufeng Formation-Longmaxi Formation

Sample	Formation	Sc	V	Cr	Co	Ni	Zn	Sr	Mo	Ba	Th	U	Zr
HSP-B1	Wufeng Formation	6.3	34	22	3.8	16.8	54	302	0.97	530	7.68	0.8	53
HSP-B2		12.2	74	40	25.5	49.5	53	127.5	1	1390	17.85	2	113
HSP-B3		5.2	30	22	7	22.5	32	338	1.31	520	7.1	0.8	60
Mean Value		7.9	46.0	28.0	12.1	29.6	46.3	255.8	1.1	813.3	10.9	1.2	75.3
Upper crust abundance		10.0	70.0	44.0	12.0	21.0	63.0	300.0	0.6	640.0	9.5	1.8	170.0
Concentration Coefficient		0.8	0.7	0.6	1.0	1.4	0.7	0.9	1.8	1.3	1.1	0.7	0.4
HSP-B4	Longmaxi Formation	14.7	80	54	4.4	26.3	80	34.2	1.86	2400	22	2.7	402
HSP-B5		16.5	102	78	4.1	34.4	73	32.6	1.01	2040	21.6	3.3	180
HSP-B6		17.8	111	83	3.7	31.1	103	41.5	1.76	2760	23.3	3.5	179
HSP-B7		16.5	157	103	3.3	60.3	150	43.3	1.45	1760	22.2	5.2	208
HSP-B8		16.1	167	108	3.7	65.2	118	40.5	1.59	1670	21.7	5.4	219
HSP-B9		10.9	121	70	1.7	26.4	31	28	0.7	1280	14.45	3.5	157
HSP-B10		12.9	143	88	2.8	43.4	60	30.1	0.89	1790	17.25	4.4	207
HSP-B11		12.6	161	128	1.3	37.4	21	39.9	1.47	1580	17.15	5	161
HSP-B12		16.9	119	85	14.8	49.7	88	32.1	3.62	1560	15.05	3.9	138
HSP-B13		16.8	122	85	4.2	43.4	95	27.3	0.75	1520	11.55	3	138
HSP-B14		17.3	117	86	3.5	43.4	97	29.6	1.26	1430	15.1	3.4	150
HSP-B15		10.8	55	44	4.7	31.2	61	45.9	0.83	350	9.73	2.2	166
Mean Value		15.0	121.3	84.3	4.4	41.0	81.4	35.4	1.4	1678.3	17.6	3.8	192.1
Upper crust abundance		10.0	70.0	44.0	12.0	21.0	63.0	300.0	0.6	640.0	9.5	1.8	170.0
Concentration Coefficient		1.5	1.7	1.9	0.4	2.0	1.3	0.1	2.4	2.6	1.9	2.1	1.1

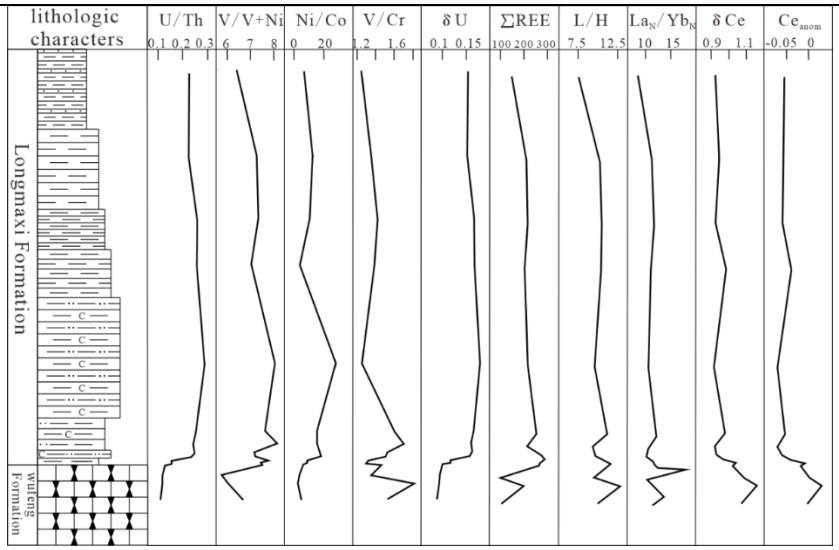

Figure 2 Vertical distribution of trace elements and rare earth elements in Wufeng-Longmaxi shale

3.3. Characteristics of rare earth element

According to the characteristic table of rock rare earth element components in the study area (table 3), the content of rare earth elements in the study area is basically consistent with the abundance of the upper crust (Gromet et al., 1985), among which La, Ce, Pr and Nd are the most enriched. According to the vertical distribution table of rare earth element index parameter ratio, the overall performance is that the bottom of Wufeng Formation and Longmaxi Formation fluctuates greatly, while the middle and top are relatively gentle, with only a small range of fluctuations. The overall performance of Longmaxi Formation is slight Ce negative anomaly.

Table 3 Characteristics of rare earth elements (μg/g) components in rock samples of Wufeng-Longmaxi Formation

	Formation	La	Ce	Pr	Nd	Sm	Eu	Gd	Tb	Dy	Ho	Er	Tm	Yb	Lu
HSP-B1	Wufeng Formation	22.90	47.60	4.95	17.70	3.41	0.63	2.68	0.47	2.71	0.50	1.49	0.22	1.35	0.21
HSP-B2		43.50	96.60	9.17	32.20	5.49	0.91	4.30	0.66	3.84	0.73	2.12	0.33	2.13	0.33
HSP-B3		20.30	42.70	4.40	15.80	3.03	0.74	2.89	0.41	2.41	0.47	1.34	0.20	1.33	0.21
Mean Value		28.90	62.30	6.17	21.90	3.98	0.76	3.29	0.51	2.99	0.57	1.65	0.25	1.60	0.25
Upper crust abundance		33.00	64.00	7.30	28.00	5.00	1.12	4.40	0.67	4.00	0.80	2.30	0.34	3.24	0.33
Concentration Coefficient		0.88	0.97	0.85	0.78	0.80	0.68	0.75	0.77	0.75	0.71	0.72	0.74	0.49	0.76
HSP-B4	Longmaxi Formation	102.50	199.00	20.70	71.00	12.70	2.37	9.95	1.51	8.31	1.45	4.11	0.61	3.77	0.59
HSP-B5		58.40	117.00	13.05	47.10	8.04	1.35	6.32	0.99	5.94	1.10	3.17	0.50	3.15	0.50
HSP-B6		57.90	119.50	13.10	45.90	7.64	1.28	5.71	0.95	5.63	1.05	3.27	0.51	3.27	0.49
HSP-B7		63.80	122.50	14.55	53.40	9.05	1.59	7.21	1.17	6.76	1.30	3.91	0.60	3.74	0.60
HSP-B8		62.50	114.00	13.90	49.70	8.69	1.57	7.19	1.12	6.77	1.37	3.99	0.65	4.11	0.64
HSP-B9		48.50	85.80	10.35	37.20	6.67	1.23	6.04	0.91	5.27	1.03	3.09	0.46	3.08	0.46
HSP-B10		60.20	109.50	12.00	43.10	7.02	1.17	5.66	0.90	5.52	1.10	3.18	0.51	3.32	0.52
HSP-B11		50.70	89.40	10.80	37.90	6.76	1.14	5.72	0.93	5.39	1.10	3.24	0.50	3.20	0.49
HSP-B12		44.20	85.70	9.89	37.80	7.08	1.31	5.23	0.80	4.82	0.90	2.67	0.40	2.67	0.40
HSP-B13		49.10	90.00	11.10	39.70	6.61	1.22	5.18	0.82	5.16	0.95	2.96	0.46	2.80	0.43
HSP-B14		49.30	89.40	10.45	37.10	6.05	1.05	4.93	0.82	5.14	0.99	3.09	0.48	2.94	0.44
HSP-B15		30.80	58.20	7.45	28.10	5.99	1.12	5.11	0.80	4.76	0.89	2.61	0.40	2.42	0.37
Mean Value		56.49	106.67	12.28	44.00	7.69	1.37	6.19	0.98	5.79	1.10	3.27	0.51	3.21	0.49
Upper crust abundance		33.00	64.00	7.30	28.00	5.00	1.12	4.40	0.67	4.00	0.80	2.30	0.34	3.24	0.33
Concentration Coefficient		1.71	1.67	1.68	1.57	1.54	1.22	1.41	1.46	1.45	1.38	1.42	1.49	0.99	1.50

4. DISCUSSION

4.1. Depositional environment

4.1.1. Palaeoclimate

The paleoclimate can affect the material source, mineral composition and element distribution of sedimentary rocks. When the rock is subjected to chemical weathering, alkali metal elements such as K, Na, and Ca are easy to cause loss, resulting in an increase in the ratio of Al2O3 to (CaO+Na2O+K2O) in the weathering products. Therefore, the chemical weathering index (CIA) can be used to indicate the paleoclimatic conditions. Its calculation formula is:

$$CIA=Al2O3/(Al2O3+CaO※+Na2O+K2O)\times 100\% \quad (1)$$

The elements in the formula are calculated by molar quantity, in which CaO※ denotes CaO from silicate. Since CaO in the sample test results is the amount of CaO in the whole rock, it is necessary to calculate it after correction. The method proposed by McLennan et al is used for correction.

The CIA values are usually 50~70 in cold and dry climates, 70~80 in warm and humid climates, and 80 ~ 100 in hot and humid climates. It can be seen from the following figure that during the Wufeng Formation period, the CIA index was below 70, the weathering intensity was weak, and it was in cold

and dry climate conditions. In the Longmaxi group, the CIA index was basically higher than 70, and showed a significant upward and downward trend.

Because the Sr element is extremely sensitive to climate change and is affected by weathering, the Rb/Sr ratio can also be used as an important basis for paleoclimate indication. The higher the Rb/Sr ratio, the more hot and humid the climatic conditions are, and the weathering intensity is severe. It can be seen from the Fig.3 that the change trend of Rb/Sr ratio is basically consistent with the change trend of CIA index, which is cold and dry in Wufeng Formation, while the paleoclimate environment of Longmaxi Formation is relatively warm and humid.

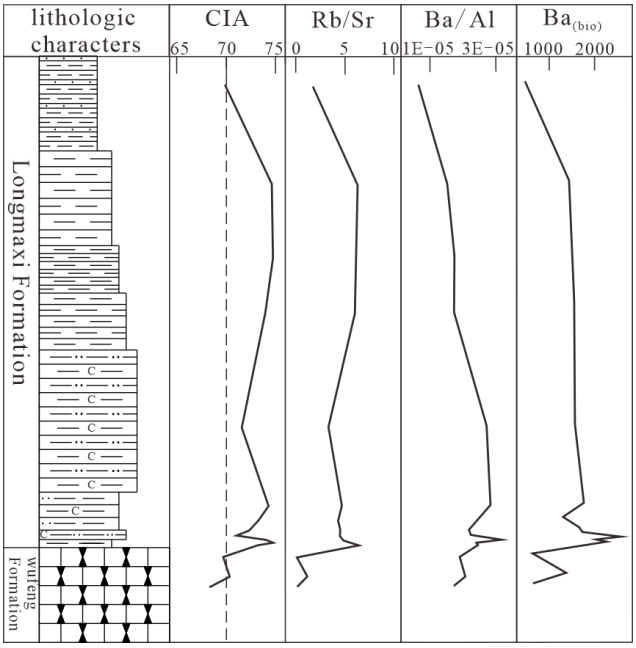

Figure 3 Vertical distribution map of paleoclimate and paleoproductivity index of Wufeng-Longmaxi Formation

4.1.2. Paleoproductivity

Paleoproductivity refers to the amount of organic matter produced by marine organisms in the geological period. Since there are four sources of Ba, the Ba/Al ratio can well reflect the level of paleoproductivity and eliminate the influence of other sources of Ba. The average value of Ba/Al in the Wufeng Formation in the study area is 1.91×10-5, and the average value of Ba/Al in the Longmaxi Formation is 2.19×10-5. Biological source Ba can directly and accurately reflect the level of productivity. The calculation formula of biological source Ba is:

$$Ba(bio)=Ba(tota1)-Ba(detrita1)=Ba(sample)-Ti(sample)\times(Ba(PAAS)\ /\ Ti(PAAS)) \quad (2)$$

In the formula, Ba(detrita1) represents Ba from terrigenous aluminosilicate sources. Through calculation, the average value of Ba(bio) in the Wufeng Formation of the study area is 812.67μg/g, while the average value of Ba(bio) in the Longmaxi Formation is 1676.96μg/g. According to the vertical variation map of Ba/Al and Ba(bio), Ba(bio) and Ba/Al values have the same distribution trend in the vertical direction, and the productivity level of Wufeng Formation is at a lower level, and the paleoproductivity level of Longmaxi Formation after the end of Henante glaciation has a higher leap. It is speculated that the sea level rises after the end of the glacial period, submerging the previously exposed and weathered surface, providing a large amount of nutrients for the ocean, and greatly improving the marine productivity.

4.1.3. Oxidation-reduction environment

The redox state is closely related to the formation of some important sedimentary minerals (such as P, Ba, Fe, U, Ni, Mo and other minerals and oil and gas), and the research significance is very

important[25, 26]. The distribution of redox-sensitive elements in sediments is dominated by their chemical properties and redox environment. Therefore, redox-sensitive elements such as V, Ni, U, Sc, Co and Cr are commonly used to determine the redox conditions of ancient oceans[27, 28]. Lewan et al. (1982) believed that V and Ni are also enriched in sediments with anoxic pore water, so they may reflect the redox conditions of the diagenesis period rather than the sedimentary period[29]. Therefore, when these elements are used to judge the redox conditions of the sedimentary environment, the influence of similar conditions should be reduced. In general, two pairs of indicators with less correlation are used for comprehensive judgment, such as V/V+Ni and Th/U intersection diagrams (Fig.4 (a)).

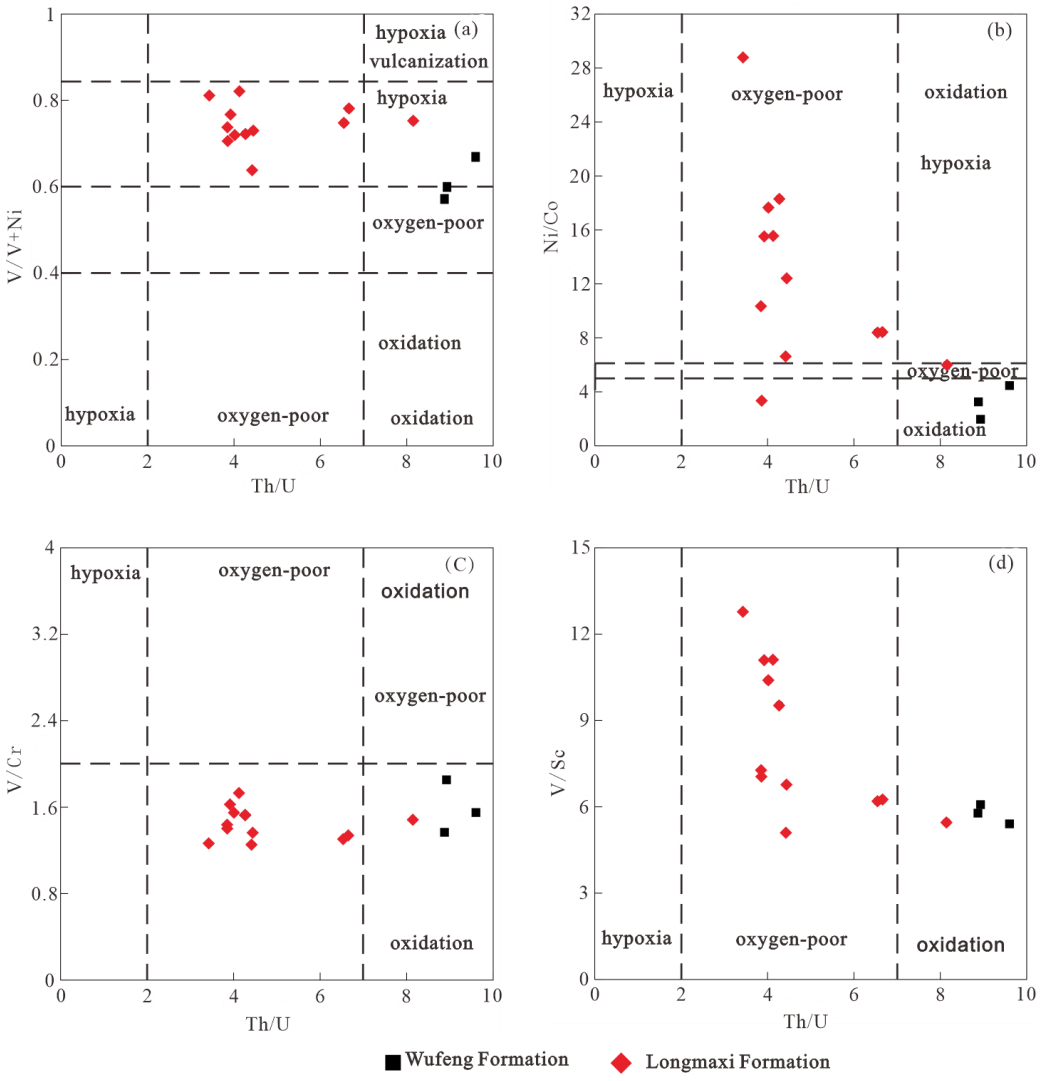

Figure 4 Wufeng-Longmaxi Formation trace element discriminant index of redox environment

Under anoxic conditions, the U element in the sediment will be enriched, while the Th element is not affected by the redox conditions of the water body, so the Th/U value can reflect the redox conditions of the sedimentary environment. In general, Th/U<2 represents an anoxic environment, 2<Th/U<7 represents an anoxic environment, and Th/U>7 represents an oxidizing condition[30]. The Th/U values of the Wufeng Formation in the study area are all greater than 7, which is an oxidizing environment, while the Longmaxi Formation is mostly between 3 and 7, representing an oxygen-poor environment. The overall performance is that the oxygen content gradually decreases from Wufeng group to Longmaxi group and then increases slightly. In addition, δU(δU=U/[1/2(U+Th/3)]) can also indicate redox conditions. When δU>1, it indicates anoxic environment. When δU<1, it is a normal seawater sedimentary environment[30]. The δU in the study area is about 0.1, with an average value

of 0.14, showing a normal seawater sedimentary environment and poor oxygen conditions. Both V and Ni are concentrated in black rock series that tend to be in a reducing environment, but their aggregation coefficients are different. Lewan (1984) pointed out that, compared with Ni, V is concentrated in a strongly reduced hydrogen sulfide-rich environment. Hatch et al.applied the V/V+Ni ratio to the study of the middle and upper Pennsylvania shale, and used it to determine the strength of the formation water stratification during sediment deposition. V/V+Ni>0.84 indicates strong stratification, 0.60 <V/V+Ni<0.84 indicates moderate stratification, and 0.40 <V/V+Ni < 0.60 indicates weak stratification[29]. The V/V+Ni in the study area is between 0.57 and 0.82, with an average of 0.72. The combination of the two indicates that the sedimentary environment is a moderately stratified bottom water body, and the circulation conditions are relatively smooth, from oxidation to reduction.

Co is dissolved in seawater in the form of Co2+ in an oxidizing environment, or forms a complex with humic acid. In the anoxic environment, insoluble CoS is formed and enters into authigenic pyrite in the form of solid solution[31]. The Ni element exists in the form of Ni2+, NiCl+ and soluble NiCO3 in the oxidizing marine environment, and also forms complexes with humic acid[31, 32]. In the absence of medium reduction intensity of H2S and manganese oxides, Ni in the organic complex will release and enter the overlying seawater or pore water. In the strong reduction environment with free H2S, Ni forms NiS insoluble and enters the authigenic pyrite in the form of solid solution[33]. These two elements will be enriched in the sediments of the reducing environment and show a certain content correlation due to the differences in their geochemical behaviors : Ni/Co<5.00 indicates the oxidizing environment 5.00<Ni/Co<7.00 indicates the anoxic environment Ni/Co>7.00 indicates the anoxic environment[30]. The Ni/Co values of the Longmaxi Formation in the study area are mostly greater than 7.00, indicating an anoxic environment. The Ni/Co values of the Wufeng Formation are less than 5.00, representing an oxidizing environment (Fig.4(b)); Both V and Cr are dissolved in water in an oxidizing environment, and are easily enriched in sediments in a reducing environment. However, there are some differences in the reduction conditions between the two. Therefore, the V/Cr value can still be used as a parameter to determine the redox environment of the ancient ocean. Jones et al. (1994) found that V/Cr<2.00 represents the oxidizing environment, 2.00<V/Cr<4.25 represents the poor oxygen environment, and V/Cr>4.25 represents the anoxic environment by studying the Upper Jurassic mudstone in the North Sea and the coast of England[30]. The V/Cr values of Wufeng Formation and Longmaxi Formation in the study area are less than 2.00, indicating an oxidizing environment (Fig.4(c)). If V is normalized by the abundance of Sc, the enrichment degree of V will be effectively presented, because the reduced V and Sc change in the same proportion in the sediment and have similar insolubility[34]. The higher the oxygen content in the environment, the lower the value of V/Sc. The V/Sc values at the bottom of the Wufeng Formation and the Longmaxi Formation in the study area are low, indicating an oxidizing environment, while the middle and top of the Longmaxi Formation show an oxygen-poor environment(Fig.4(d)).

Ce element is a variable valence element. Under oxidation conditions, Ce is oxidized from a trivalent soluble state to a tetravalent insoluble state. The loss degree of Ce can well reflect the redox environment. δCe value(δCe=CeN/(LaN×PrN)1/2 The higher the δCe is, the more Ce is oxidized and deposited, indicating that the higher the oxygen content in the environment ; on the contrary, the environment is closer to the reduction condition[35]. Similarly, the Ce anomaly index can also be used to determine the redox environment of the water body. The calculation formula of the Ce anomaly index is[36]:

$$Ceanom=Lg[3CeN/(2LaN+NdN)] \quad (3)$$

Ceanom>-0.1 indicates the oxidation environment, Ceanom<-0.1 represents the reduction environment. The δCe values of the samples in the study area are between 0.92 and 1.16, with an average of 1.00. According to the vertical distribution map of rare earth elements, the samples of Wufeng Formation have δCe>1, and Ce elements are enriched, indicating an oxidizing environment, while most samples of Longmaxi Formation have δCe<1, and Ce elements are slightly depleted,

showing an oxygen-poor environment. The Ceanom index is between -0.07 and 0.03. The average value of Ceanom index in Wufeng formation is 0.01, which is a positive anomaly. The average value of Ceanom index in Longmaxi formation is -0.05. In its vertical distribution diagram (Fig.2), δCe and Ceanom index show the same characteristics, that is, the oxygen content of Wufeng formation is higher than that of Longmaxi formation.

In summary, the water body in the Wufeng Formation was an oxidizing environment during deposition, and the water body was shallow, while the water body in the Longmaxi Formation was deep, which was an oxygen-poor reducing environment.

4.1.4. Rate of sedimentation

The rare earth elements are mainly deposited into the ocean with suspended solids and detrital minerals. When the suspended solids and detrital minerals are deposited in the sea water for a shorter time, the deposition rate is faster, the degree of differentiation of rare earth elements is lower, the REE distribution curve is more gentle, and Ce is positive or weak negative anomaly.

The LaN/YbN ratio can well reflect the degree of differentiation of rare earth elements, and the ratio can roughly represent the degree of differentiation of rare earth elements, which can reflect the speed of deposition rate. The average value of LaN/YbN in the Wufeng Formation in the study area is 11.8, and the average value of LaN/YbN in the Longmaxi Formation is 11.7. The vertical distribution map of LaN/YbN indicates that the deposition rate in the Wufeng Formation is faster (Fig.5). There is a layer with a very slow deposition rate at the bottom of the Longmaxi Formation, and then the deposition rate begins to accelerate. At the same time, the Ceanom vertical change map also reflects this situation. At the bottom of the Longmaxi Formation, Ce is weakly negative anomaly, reflecting that the deposition rate is relatively slow at this layer. The weak negative anomaly or even positive anomaly of Ce in the Wufeng Formation is speculated to be affected by the oxidation environment during the deposition of the Wufeng Formation, resulting in Ce enrichment. The change of deposition rate has a great relationship with the paleogeographic environment at the time of deposition. During the geological history period of Late Ordovician-Early Silurian, global glacial events, marine anoxic events and biological extinction events occurred around the world. Among them, the Hirnantian glacial period caused a significant decrease in global sea level and a significant increase in water deposition rate. After the glacial period, the deposition rate began to decline. This slow deposition rate during the deposition of the early strata of the Longmaxi Formation can reflect this historical event.

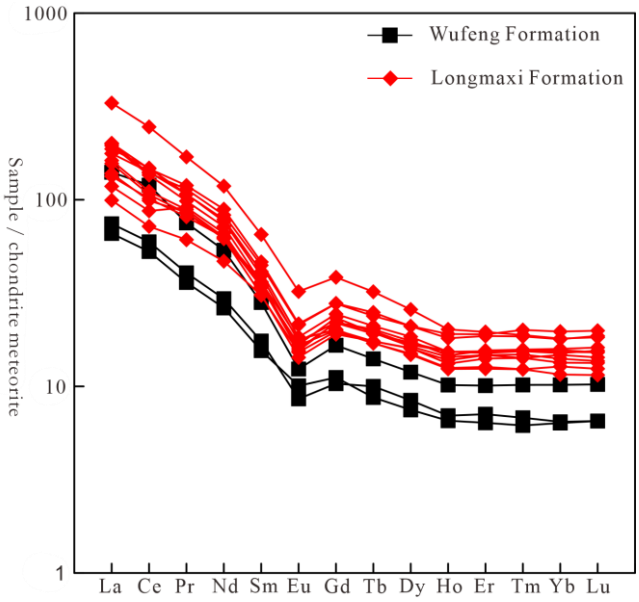

Figure 5 Wufeng-Longmaxi Formation Shale REE distribution patterns (chondrite normalized according to Taylor and Mclennan, 1985)

4.1.5. Basin water retention degree

The retention degree of seawater in the basin is an important feature of the marine system, which can affect the sedimentary environment and biogeochemical cycle in the ocean. It is mainly affected by sea level rise and tectonic movement. Due to the retention of water in the basin, resulting in water hypoxia, such an environment is conducive to the preservation of organic matter. Because the geochemical behavior of U and Mo in anoxic environment is quite different : the uptake of U in sediments is earlier than that of Mo, manganese and iron hydroxides will accelerate the speed of Mo entering the sediments without affecting U. Based on these two different geochemical characteristics and the study of barrier anaerobic basins this year, many scholars have proposed to use the U-Mo covariation model in sediments to determine the retention of water bodies[31, 37].

The U-Mo covariation model can simultaneously distinguish the retention degree and redox environment of the sea basin water. For the use of U-Mo covariant model, the concept of enrichment factor (EFelement) needs to be introduced. The calculation formula of enrichment factor is:

$$EFelement=(element/Al)sample/(element/Al)PAAS \quad (4)$$

An EFelement<1 indicates that the element is depleted relative to the average marine shale, and vice versa. Tribovillard distinguished three kinds of U-Mo covariant models in non-retention, weak-retention and strong-retention marine environments through the study of modern basins[33]. It can be seen from the Fig.6 that for the samples with TOC<2% in the Longmaxi Formation, the falling point is between 0.3×SW and 1×SW, showing a medium retention environment, while for the samples with TOC>2%, the sedimentary environment is a strong retention environment of modern marine type (Black Sea).

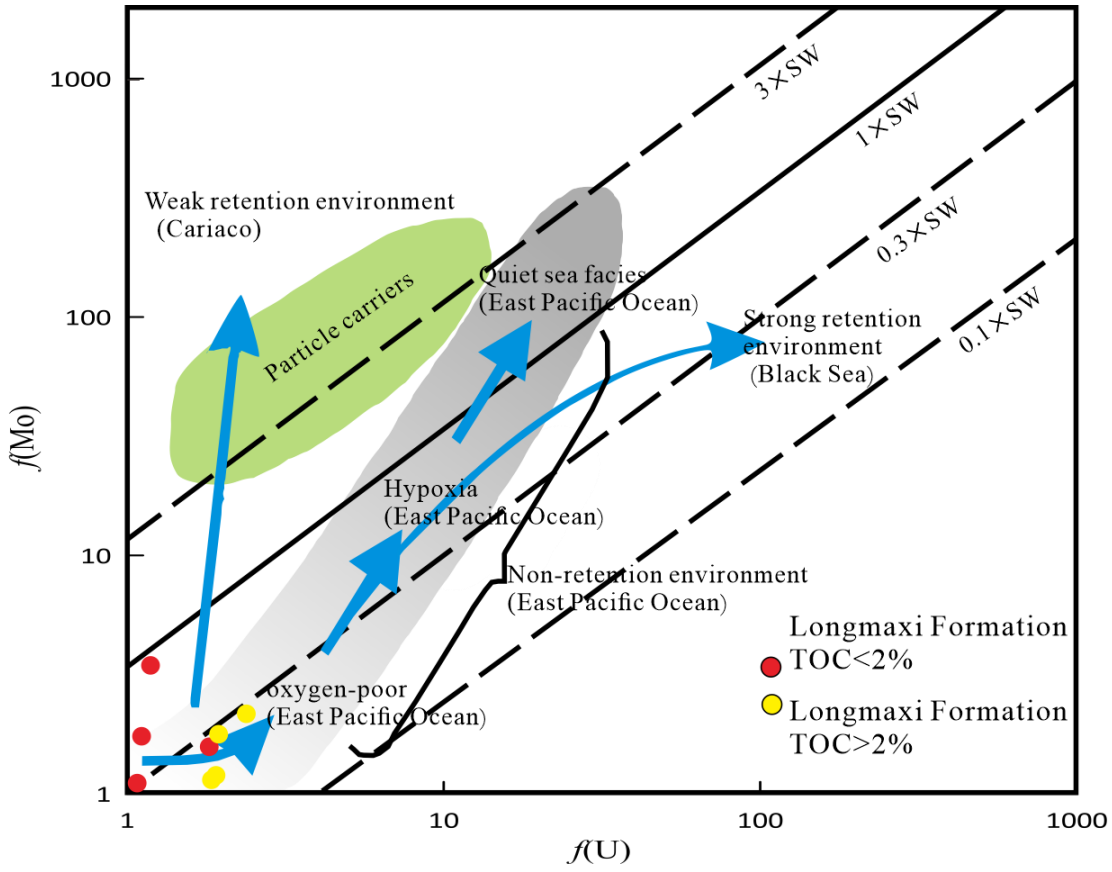

Figure 6 Longmaxi Formation U-Mo covariant diagram

4.2. Background of source region

4.2.1. Provenance analysis

Rare earth elements can well retain the geochemical information of the source area, and the materials from the same source often have similar rare earth element distribution pattern curves. Therefore, rare earth elements can be used as indicators for provenance analysis[38]. The samples in the study area were chondrite-normalized. From the rare earth element distribution pattern map (Fig.5), it can be seen that the rare earth element distribution patterns of the Wufeng Formation and the Longmaxi Formation are basically the same, both of which are right-leaning patterns, and there are Eu negative anomalies and slight Ce anomalies, which are consistent with the rare earth element distribution characteristics of the upper crust. It shows that the source of the sediments of the Wufeng Formation and the Longmaxi Formation in the study area is the upper crustal material. There is a little fluctuation in the distribution coefficient curve of Wufeng Formation, indicating that there is a mixture source in its deposition. The overall distribution pattern of the Longmaxi Formation is relatively consistent, indicating that the source is single during deposition, but there is a large fluctuation in the No.4 sample at the bottom of the observation section. The deposition of this part was input by other sources.

La/Yb-∑REE diagram can be used to determine the provenance lithology[39]. It can be seen from the Fig.7 that the samples of Wufeng Formation fall in the sedimentary rock-calcareous mudstone area, while the samples of Longmaxi Formation fall in the granite area and both of them have some samples falling outside the area. In the La/Sc-Co/Th diagram, most of the samples of Wufeng Formation and Longmaxi Formation fall in the felsic volcanic rock source area, which indicates that there are some mixed sources of sedimentary process. This is consistent with the conclusion of the rare earth element distribution pattern curve, and the source rock in the study area is mainly felsic granite.

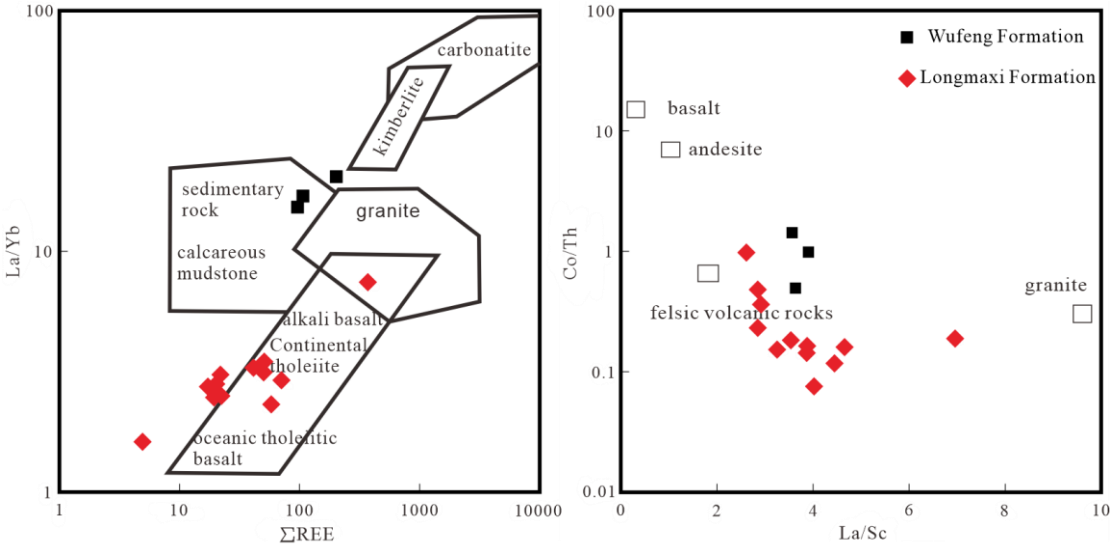

Figure 7 Wufeng-Longmaxi Formation shale La/Yb-∑REE and La/Sc-Co/Th diagram

Submarine hydrothermal fluid plays an important role in the deposition of black rock series[40]. The Ba/Sr value can be used to distinguish the submarine hydrothermal activity : the Ba/Sr value in normal marine sedimentary rocks is 1, and the larger the Ba/Sr value, the stronger the influence of submarine hydrothermal activity[41]. The Ba/Sr values of the Longmaxi Formation samples in the study area are all >1. It indicates that it is affected by certain submarine hydrothermal activity during deposition.

The influence of hydrothermal solution can also be determined by the Zn-Ni-Co triangle diagram[42]. The Fig.8 shows that the Wufeng Formation and the Longmaxi Formation in the study area were affected by submarine hydrothermal deposition or hydrothermal altered crust. The contribution of seawater and seafloor hydrothermal fluids can be distinguished by the Eu/Sm-Sm/Yb binary mixing

model[43]. It can be seen from the Fig.8 that the Wufeng Formation and Longmaxi Formation in the study area are close to the hydrous ferromanganese crust, and the proportion of submarine hydrothermal fluid in the original solution is less than 0.1 %.

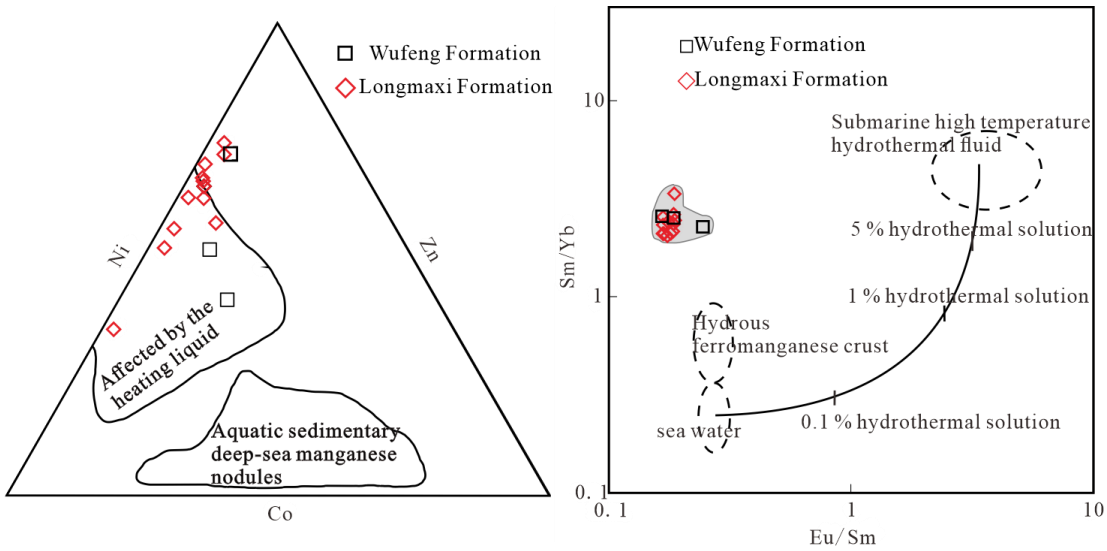

Figure 8 Source discrimination diagram of Zn-Ni-Co and Eu/Sm-Sm/Yb diagram of Wufeng-Longmaxi shale

4.2.2. Tectonic setting analysis

The geochemical characteristics of elements are different under the influence of different tectonic backgrounds. The inversion of tectonic background in the sedimentary process can use the characteristics of rare earth elements as indicators. Reference to Bhatia (1985) listed under different tectonic setting of mixed sandstone rare earth element characteristics and ratio range table. Because mudstone samples have higher rare earth element content than sandstone samples, it is necessary to divide the element value of mudstone by 1.2 for correction, so as to obtain the rare earth element content equivalent to sandstone in the same period[44]. The corrected rare earth element content of the samples was compared with that of the samples. The results show that the corrected values of La, Ce, ∑REE, ∑LREE/∑HREE and Eu/Eu* of the Wufeng Formation samples in the study area are close to the continental island arc, and the corrected values of La/Yb and LaN/YbN are close to the passive continental margin. The ∑REE, La/Yb, LaN/YbN, and La, Ce correction values of the Longmaxi Formation samples in the study area are close to the passive continental margin, and the ∑LREE/∑HREE and Eu/Eu* correction values are close to the active continental margin. The tectonic background of the Wufeng Formation is close to the continental island arc, while the tectonic background of the Longmaxi Formation is close to the passive continental margin.

Table 4 Comparison of REE characteristics between the samples in the study area and the greywacke in sedimentary basins with different tectonic backgrounds.

tectonic setting	La	Ce	∑REE	La/Yb	LaN/YbN	∑LREE/∑HREE	Eu/Eu*
oceanic island	8±1.7	19±3.7	58±10	4.2±1.3	2.8±0.9	3.8±0.9	1.04±0.11
continental island arc	27±4.5	59±8.2	146±20	11.0±3.6	7.5±2.5	7.7±1.7	0.79±0.13
active continental margins	37	78	186	12.5	8.5	9.1	0.6
passive continental margin	39	85	210	15.9	10.8	8.5	0.56
In the study area Wufeng Formation Mean Value	28.90	62.30	135.12	17.55	11.83	10.83	0.64
corrected value	24.08	51.92	112.60	17.55	11.83	10.83	0.64
In the study area Longmaxi Formation Mean Value	56.49	106.67	250.03	17.42	11.74	10.47	0.59
corrected value	47.08	88.89	208.36	17.67	11.76	10.54	0.59

The combination of rare earth elements and trace elements with strong stability can also be used to distinguish the tectonic background[45]. The tectonic background analysis is carried out according to La-Th-Sc, Th-Sc-Zr/10 and Th-Co-Zr/10 plates. It can be seen from Fig.9 that the landing points of the Wufeng Formation samples are basically consistent, which is an active continental margin. Most of the Longmaxi Formation also falls on the active continental margin, and a few fall on the continental island arc. It shows that the sedimentary tectonic background of the study area in Ordovician-Silurian is mainly active continental margin. It shows that the collision between the Ordovician-Silurian Huaxia plate and the Yangtze plate is still occurring.

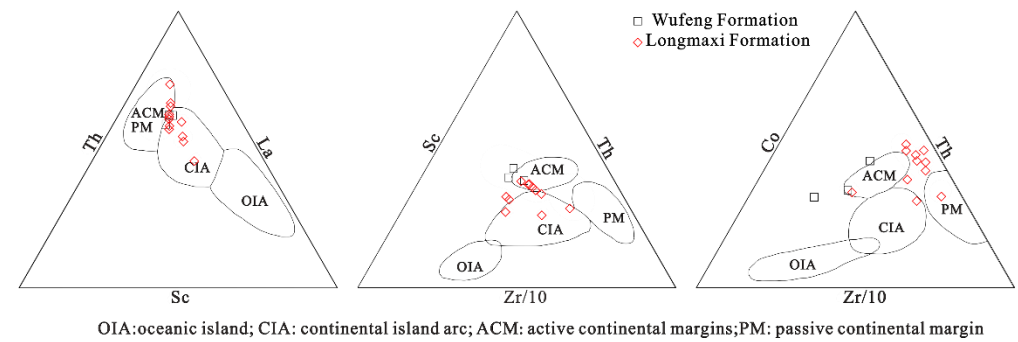

Figure 9 Wufeng-Longmaxi Formation Construct background discriminant diagram

5. CONCLUSIONS

(1) According to the CIA index, it can be judged that the paleoclimate of the Wufeng Formation in the study area was cold and dry, and the paleoclimate of the Longmaxi Formation was warm and humid. The Ba/Al ratio and Ba(bio) show high paleoproductivity at the bottom of Longmaxi.

(2) According to the indicators of redox sensitive elements, it is shown that the Wufeng Formation in the study area is oxidized-oxygen-poor environment, and the Longmaxi Formation is oxygen-poor-anoxic environment.

(3) The differentiation degree of rare earth elements reflects that the deposition rate of Wufeng Formation is faster, while there is a region with slower deposition rate at the bottom of Longmaxi Formation.

(4) The U-Mo covariation model shows that the water retention of Longmaxi Formation is at a level from strong retention to medium retention.

(5) The source material of Wufeng Formation in the study area comes from the upper crust, and the source rock is mainly felsic granite. During the deposition, it is affected by a small amount of hydrothermal fluid. The sedimentary tectonic background has been mainly active continental margin, and it also shows some continental island arc tectonic background.

CONFLICTS OF INTEREST

The authors declare that they have no conflict of interest.

ACKNOWLEDGEMENTS

This work was sustained by the Hubei Shale Gas Development Co., Ltd (No. HBYYQ–GC1075).

REFERENCES

[1] Lu, Y.; Hao, F.; Ma, Y.; Wei, W.; Jun, S.; Wang, Y.; Gou, Q., Spatial heterogeneity in salinity and redox dynamics during the Ordovician-Silurian transition: Multi-proxy constraints on the Late Ordovician Mass Extinction mechanisms. Chemical Geology 2025, 690, 122860. https://doi.org/10.1016/j.chemgeo.2025.122860

[2] Yang, X.; Yan, D.; Wilson, D. J.; Pogge Von Strandmann, P. A. E.; Liu, X.; Liu, C.; Tian, H.; Liu, M.; Zhang, L.; Zhang, B.; Chen, D., Lithium isotope and mercury evidence for enhanced continental weathering and intense volcanism during the Ordovician-Silurian transition. Geochimica et Cosmochimica Acta 2025, 391, 49-68. https://doi.org/10.1016/j.gca.2024.12.010

[3] Halsey, T.; Agrawal, G.; Bailey, J. R.; Balhoff, M.; Borglum, S.; Mohanty, K. K.; Traver, M., Grand Challenges for the Oil and Gas Industry for the Next Decade and Beyond. JPT, Journal of Petroleum Technology 2023, 75, (7), 52-56. 10.2118/0723-0052-JPT

[4] Wang, S.; Man, L.; Wang, S.; Wu, L.; Zhu, Y.; Li, Y.; He, Y., Lithofacies types, reservoir characteristics and silica origin of marine shales: A case study of the Wufeng formation–Longmaxi Formation in the Luzhou area, southern Sichuan Basin. Natural Gas Industry B 2022, 9, (4), 394-410. https://doi.org/10.1016/j.ngib.2022.07.004

[5] Cui, Y.; Li, X.; Han, L.; Guo, W.; Lin, W.; Chang, R.; Shen, W.; Huang, Y.; Qian, C., Organic Matter Enrichment of Black Shale at the Turn of Ordovician-Silurian in the Paleosedimentary Center in Southern Sichuan Basin, Upper Yangtze Area. Lithosphere 2022, 2022, (SpecialIssue12). 10.2113/2022/6809092

[6] Wu, Y.; Fan, T.; Zhang, J.; Jiang, S.; Li, Y.; Zhang, J.; Xie, C., Characterization of the upper ordovician and lower silurian marine shale in northwestern guizhou province of the upper yangtze block, South China: Implication for shale gas potential. Energy and Fuels 2014, 28, (6), 3679-3687. 10.1021/ef5004254

[7] Jiang, S.; Zhou, Q.; Li, Y.; Ji, A.; Chen, Z.; Yang, R.; Zhu, X.; Chao, H., Reservoir characteristics and gas-bearing property of Wufeng-Longmaxi shale in well HY2, Hefeng area. Arabian Journal of Geosciences 2022, 15, (8), 775. 10.1007/s12517-022-10020-w

[8] Hao, Y.; Wu, L.; Jiang, W.; Qian, C.; Zhou, X.; Wang, Y., Development characteristics and controlling mechanism of different microfracture combinations in shale reservoir: A case study of Silurian Longmaxi Formation in Weiyuan area. Petroleum Research 2025, 10, (1), 66-78. https://doi.org/10.1016/j.ptlrs.2024.07.003

[9] Jiang, S.; Zhou, Q.; Li, Y.; Ji, A.; Chen, Z.; Yang, R.; Zhu, X.; Chao, H., Reservoir characteristics and gas-bearing property of Wufeng-Longmaxi shale in well HY2, Hefeng area. Arabian Journal of Geosciences 2022, 15, (8), 775. 10.1007/s12517-022-10020-w

[10] Xie, G. G.; Xie, G. L.; Jiao, K., Multi-fractal characteristics of pore system in deep organic-rich shales of the Wufeng-Longmaxi formation in the Sichuan Basin and their geological significance. FRONTIERS IN EARTH SCIENCE 2024, 12. 10.3389/feart.2024.1430466

[11] Ye, Y. P.; Tang, S. H.; Xi, Z. D.; Lin, D. L.; Shen, Y. Y., Factors Controlling Brittleness of the Wufeng-Longmaxi Shale in the Yangtze Platform, South China: Insights from Geochemistry and Shale Composition. ENERGY & FUELS 2022, 36, (18), 10945-10959. 10.1021/acs.energyfuels.2c02329

[12] Zou, Z. W.; Fu, J. H.; Li, H.; Liu, Y. Y.; Zhang, C. L.; Xia, Z. Q.; Fan, C. H., Controlling factors for shale gas enrichment and their implications for favorable exploration areas: Insights from the Wufeng-Longmaxi Formations, Southern Sichuan, China. PLOS ONE 2025, 20, (5). 10.1371/journal.pone.0323277

[13] Wang, Z.; Yang, F.; Liu, J.; Yang, P.; Deng, Q.; Xiong, X., Sedimentary transformation of the Wufeng-Longmaxi Formation and its geologic significances of shale gas in Northeast Yunnan. Sedimentary Geology and Tethyan Geology 2020, 40, (3), 129-139. 10.19826/j.cnki.1009-3850.2020.07006

[14] Yi, X. F.; Ji, X.; Huang, Y. F.; Liu, Z. S.; Meng, J. H., Black Shale Paleo-Environmental Reconstructions: A Geochemical Case Study of Two Ordovician-Silurian Boundary Sections in Middle Yangtze Area, China. FRONTIERS IN EARTH SCIENCE 2022, 10. 10.3389/feart.2022.842752

[15] ZHANG, H.; XU, X.; LIU, W.; MEN, Y., Late Ordovician-Early Silurian sedimentary facies and palaeogeographic evolution and its bearings on the black shales in the Middle-Upper Yangtze area. Sedimentary Geology and Tethyan Geology 2013, 33, (2), 17-24.

[16] Chen, X.; Fan, J.; Chen, Q.; Tang, L.; Hou, X., Toward a stepwise Kwangsian Orogeny. Science China Earth Sciences 2014, 57, (3), 379-387. 10.1007/s11430-013-4815-y

[17] Qiu, Z.; Li, Y.; Xiong, W.; Fan, T.; Zhao, Q.; Zhang, Q.; Wang, Y.; Liu, W.; Liang, F.; Zhang, J.; Lash, G., Revisiting paleoenvironmental changes on the Upper Yangtze Block during the Ordovician-Silurian transition: New insights from elemental geochemistry. Sedimentary Geology 2023, 450, 106377. https://doi.org/10.1016/j.sedgeo.2023.106377

[18] Shi, Z.; Yuan, Y.; Zhao, Q.; Sun, S.; Zhou, T.; Cheng, F., Paleogeomorphology and shale distribution of Late Ordovician-Early Silurian Yangtze platform, South China: Implication for shale mineralogy and TOC content. Journal of Natural Gas Geoscience 2023, 8, (4), 245-262. https://doi.org/10.1016/j.jnggs.2023.06.001

[19] Yan, D.; Wang, Q., Sedimentary environment and development controls of the hydrocarbon sources beds: The Upper Ordovician Wufeng Formation and the Lower Silurian Longmaxi Formation in the Yangtze area. Acta Geologica Sinica(English Edition) 82, (3).

[20] Chen, X.; Fan, J.; Chen, Q.; Tang, L.; Hou, X., Toward a stepwise Kwangsian Orogeny. Science China Earth Sciences 2014, 57, (3), 379-387. 10.1007/s11430-013-4815-y

[21] DENG Xin, Y. K. L. P., Characteristics and tectonic evolution of Qianzhong Uplift. Earth Science Frontiers 2010, 17, (3), 79-89.

[22] Zhou, Z.; Zhou, H.; Jiang, Z. X.; Li, S. Z.; Bao, S. J.; Xu, G. H., The Range and Evolution Model of the Xiang-E Submarine Uplifts at the Ordovician-Silurian Transition: Evidence from Black Shale Graptolites. JOURNAL OF MARINE SCIENCE AND ENGINEERING 2025, 13, (4). 10.3390/jmse13040739

[23] Diao, Z.; Huo, F.; Li, P., Characterization of shale pore heterogeneity and its controlling factors: A case study of the Longmaxi Formation in Western Hubei, China. Energy Science and Engineering 2024, 12, (7), 2899-2917. 10.1002/ese3.1782

[24] Gromet, L. P.; Haskin, L. A.; Korotev, R. L.; Dymek, R. F., The "North American shale composite": Its compilation, major and trace element characteristics. Geochimica et Cosmochimica Acta 1984, 48, (12), 2469-2482. https://doi.org/10.1016/0016-7037(84)90298-9

[25] Francois, R., A study on the regulation of the concentrations of some trace metals (Rb, Sr, Zn, Pb, Cu, V, Cr, Ni, Mn and Mo) in Saanich Inlet Sediments, British Columbia, Canada. Marine Geology 1988, 83, (1), 285-308. https://doi.org/10.1016/0025-3227(88)90063-1

[26] Russell, A. D.; Morford, J. L., The behavior of redox-sensitive metals across a laminated–massive–laminated transition in Saanich Inlet, British Columbia. Marine Geology 2001, 174, (1), 341-354. https://doi.org/10.1016/S0025-3227(00)00159-6

[27] Abanda, P. A.; Hannigan, R. E., Effect of diagenesis on trace element partitioning in shales. Chemical Geology 2006, 230, (1), 42-59. https://doi.org/10.1016/j.chemgeo.2005.11.011

[28] Crusius, J.; Calvert, S.; Pedersen, T.; Sage, D., Rhenium and molybdenum enrichments in sediments as indicators of oxic, suboxic and sulfidic conditions of deposition. Earth and Planetary Science Letters 1996, 145, (1), 65-78. https://doi.org/10.1016/S0012-821X(96)00204-X

[29] Lewan, M. D.; Maynard, J. B., Factors controlling enrichment of vanadium and nickel in the bitumen of organic sedimentary rocks. Geochimica et Cosmochimica Acta 1982, 46, (12), 2547-2560. https://doi.org/10.1016/0016-7037(82)90377-5

[30] Jones, B.; Manning, D. A. C., Comparison of geochemical indices used for the interpretation of palaeoredox conditions in ancient mudstones. Chemical Geology 1994, 111, (1), 111-129. https://doi.org/10.1016/0009-2541(94)90085-X

[31] Algeo, T. J.; Rowe, H., Paleoceanographic applications of trace-metal concentration data. Chemical Geology 2012, 324-325, 6-18. https://doi.org/10.1016/j.chemgeo.2011.09.002

[32] Calvert, S. E.; Pedersen, T. F., Geochemistry of Recent oxic and anoxic marine sediments: Implications for the geological record. Marine Geology 1993, 113, (1), 67-88. https://doi.org/10.1016/0025-3227(93)90150-T

[33] Tribovillard, N.; Algeo, T. J.; Lyons, T.; Riboulleau, A., Trace metals as paleoredox and paleoproductivity proxies: An update. Chemical Geology 2006, 232, (1), 12-32. https://doi.org/10.1016/j.chemgeo.2006.02.012

[34] Kimura, H.; Watanabe, Y., Oceanic anoxia at the Precambrian-Cambrian boundary. Geology 2001, 29, (11), 995.

[35] Berry, W. B. N.; Wilde, P., PROGRESSIVE VENTILATION OF THE OCEANS - AN EXPLANATION FOR THE DISTRIBUTION OF THE LOWER PALEOZOIC BLACK SHALES. 1978, 278, (3), 257-275. 10.2475/ajs.278.3.257

[36] Elderfield, H.; Greaves, M. J., The rare earth elements in seawater. Nature 1982,.

[37] Algeo, T. J.; Tribovillard, N., Environmental analysis of paleoceanographic systems based on molybdenum–uranium covariation. Chemical Geology 2009, 268, (3), 211-225. https://doi.org/10.1016/j.chemgeo.2009.09.001

[38] Bhatia, M. R., Rare earth element geochemistry of Australian Paleozoic graywackes and mudrocks: Provenance and tectonic control. Sedimentary Geology 1985, 45, (1), 97-113. https://doi.org/10.1016/0037-0738(85)90025-9

[39] Allègre, C. J.; Minster, J. F., Quantitative models of trace element behavior in magmatic processes. Earth and Planetary Science Letters 1978, 38, (1), 1-25. https://doi.org/10.1016/0012-821X(78)90123-1

[40] Yu, B.; Dong, H.; Widom, E.; Chen, J.; Lin, C., Geochemistry of basal Cambrian black shales and cherts from the Northern Tarim Basin, Northwest China: Implications for depositional setting and tectonic history. Journal of Asian Earth Sciences 2009, 34, (3), 418-436. https://doi.org/10.1016/j.jseaes.2008.07.003

[41] Peter, J. M.; Scott, S. D., Mineralogy, composition, and fluid-inclusion microthermometry of seafloor hydrothermal deposits in the Southern Trough of Guaymas Basin, Gulf of California. Canadian Mineralogist 1988, 26 pt 3, 567-587.

[42] Choi, J. H.; Hariya, Y., Geochemistry and depositional environment of Mn oxide deposits in the Tokoro Belt, northeastern Hokkaido, Japan. Economic Geology 1992, 87, (5), 1265-1274.

[43] Alexander, B. W.; Bau, M.; Andersson, P.; Dulski, P., Continentally-derived solutes in shallow Archean seawater: Rare earth element and Nd isotope evidence in iron formation from the 2.9Ga Pongola Supergroup, South Africa. Geochimica et Cosmochimica Acta 2008, 72, (2), 378-394. https://doi.org/10.1016/j.gca.2007.10.028

[44] Condie, K. C., Chemical composition and evolution of the upper continental crust: Contrasting results from surface samples and shales. Chemical Geology 1993, 104, (1), 1-37. https://doi.org/10.1016/0009-2541(93)90140-E

[45] Bhatia, M. R.; Crook, K. A. W., Trace element characteristics of graywackes and tectonic setting discrimination of sedimentary basins. Contributions to Mineralogy and Petrology 1986, 92.